



Published in final edited form as:

J Proteome Res. 2010 February 5; 9(2): 865–875. doi:10.1021/pr900761m.

Association of Immunosuppressant-induced Protein Changes in the Rat Kidney with Changes in Urine Metabolite Patterns: A Proteo-Metabonomic Study

Jost Klawitter^{1,2,3,*}, Jelena Klawitter^{1,3,*}, Erich Kushner¹, Karen Jonscher¹, Jamie Bendrick-Peart², Dieter Leibfritz³, Uwe Christians¹, and Volker Schmitz^{1,4}

¹Department of Anesthesiology, University of Colorado Denver, Aurora, CO, USA

²Eurofins Medinet Denver, Aurora, CO, USA

³Institut für Organische Chemie, Universität Bremen, Bremen, Germany

⁴Department of General-, Visceral- and Transplantation Surgery, Charité, Campus Virchow, Berlin, Germany

Abstract

The basic mechanisms underlying calcineurin inhibitor (CI) nephrotoxicity and its enhancement by sirolimus are still largely unknown. We investigated the effects of CIs alone and in combination with sirolimus on the renal proteome and correlated these effects with urine metabolite pattern changes.

Thirty-six male Wistar rats were assigned to six treatment groups (n=4/group for proteome analysis and n=6/group for urine ¹H-NMR metabolite pattern analysis): vehicle controls, sirolimus 1mg/kg/day, cyclosporine 10mg/kg/day, cyclosporine 10mg/kg/day + sirolimus 1mg/kg/day, tacrolimus 1mg/kg/day, tacrolimus 1mg/kg/day + sirolimus 1mg/kg/day. After 28 days, 24h-urine was collected for ¹H-NMR-based metabolic analysis and kidneys were harvested for 2D-gel electrophoresis and histology.

Cyclosporine affected the following groups of proteins: calcium homeostasis (regucalcin, calbindin), cytoskeleton (vimentin, caldesmon), response to hypoxia and mitochondrial function (prolyl 4-hydroxylase, proteasome, NADH dehydrogenase) and cell metabolism (kidney aminoacylase, pyruvate dehydrogenase, fructose-1,6-bis phosphate). Several of the changes in protein expression, confirmed by Western blot, were associated with and explained changes in metabolite concentrations in urine. Representative examples are an increase in kidney aminoacylase expression (decrease of hippurate concentrations in urine), up regulation of pyruvate dehydrogenase and fructose-1, 6-bisphosphatase, (increased glucose metabolism) and down regulation of arginine:glycine-amidino transferase (most likely due to an increase in creatinine concentrations).

Protein changes explained and qualified immunosuppressant-induced metabolite pattern changes in urine.

*Corresponding Author: Jost Klawitter, PhD, University of Colorado Denver, Department of Anesthesiology, 1999 North Fitzsimons Parkway, Bioscience East Suite 100, 80045 Aurora, Colorado, USA, jost.klawitter@ucdenver.edu, Phone: 720 961 4483, Fax: 303 724 5662.

*both authors have contributed equally to this work

Keywords

Cyclosporine; sirolimus; tacrolimus; kidney dysfunction markers; immunosuppressants; metabolomics; proteomics; nephrotoxicity; regucalcin; calbindin

Introduction

Calcineurin inhibitors such as cyclosporine and tacrolimus are the basis of most immunosuppressive protocols following organ transplantation (1, 2). While these drugs protect transplant organs from rejection, they may also cause organ damage, especially in the kidney. In fact, calcineurin inhibitor induced nephrotoxicity has been identified as the major cause of kidney dysfunction following transplantation of non-renal solid organs (3). Sirolimus is an immunosuppressive agent that inhibits the mammalian target of rapamycin (mTOR inhibitor) and synergistically augments immunosuppression when combined with calcineurin inhibitors. This makes it possible to use lower doses of both combination partners and results in better short-term outcome following transplantation (4). Although devoid of nephrotoxicity when administered alone, Sirolimus can enhance the negative effects of cyclosporine on kidney function (5–8).

Chronic immunosuppressant-mediated nephrotoxicity is a significant concern. Graft loss due to calcineurin inhibitor toxicity must be regarded as unacceptable, particularly in light of the increasing disparity between organ supply and demand. While acute immunosuppressant toxicity is usually associated with increased drug exposure and is easily detected, diagnosis of chronic toxicity proves a more challenging task (9). Reducing or avoiding the negative effects of chronic immunosuppressant toxicity rely on early detection and individualization of immunosuppressive drug regimens (10).

As of today, the basic biochemical mechanisms of calcineurin inhibitors toxicity remain largely unknown. It is therefore unclear if inhibition of calcineurin and/or cyclophilins/ FK-binding proteins, the molecular targets of cyclosporine and tacrolimus that are responsible for its immunosuppressive activity, play a key role in the mediation of their toxicities (11). The only studies examining the mechanisms responsible for the enhancement of cyclosporine nephrotoxicity by sirolimus are limited to pharmacokinetic drug interaction studies (8), and there are no studies evaluating the potential of molecular mechanisms enhancing the toxicity of calcineurin inhibitor tacrolimus by sirolimus.

In previous studies (12, 13) we have shown that the negative effects on the kidney by cyclosporine and sirolimus, alone or in combination, are reflected by changes of the metabolite patterns in urine. These studies revealed that after 28 days of cyclosporine treatment, urine metabolite patterns typical for proximal tubular damage were observed. This included the reduction of Krebs cycle intermediates and trimethylamine-N-oxide concentrations whereas the concentrations of acetate, lactate, trimethylamine and glucose were increased. Sirolimus enhanced these negative effects. It is reasonable to expect that the profiling of metabolite and protein expression in the kidney will reveal critical mechanistic information about the nephrotoxic effects of calcineurin inhibitors. In this study we employed a combination of non-targeted proteomics and metabolic profiling in the kidney tissue and urine of rats treated with calcineurin inhibitors alone or in combination with sirolimus for 28 days. We then correlated these results with tissue pathology (histology) and clinically relevant kidney function parameters such as creatinine concentrations in serum and glomerular filtration rates. It was the goal of the present study (A) to further assess the molecular mechanisms underlying immunosuppressive drug toxicity and to compare the effects of the calcineurin inhibitors cyclosporine and tacrolimus alone and in combination

with sirolimus, (B) to explain and qualify the associated metabolite pattern changes in urine by linking the urine metabolite changes to immunosuppressant-induced changes in protein expression in the kidney and (C) to discover new potential protein molecular markers of immunosuppressant toxicity in kidney tissue.

Methods

Animals

Thirty-six male Wistar rats were acclimatized for two weeks and then randomly assigned to six treatment groups (n=4/group for proteomics and n=6/group for urine ¹H-NMR analysis):

- I. vehicle controls 28 days
- II. sirolimus 1 mg/kg/day for 28 days
- III. tacrolimus 1 mg/kg/day for 28 days
- IV. tacrolimus 1 mg/kg/day + sirolimus 1 mg/kg/day for 28 days
- V. cyclosporine 10 mg/kg/day for 28 days
- VI. cyclosporine 10 mg/kg/day + sirolimus 1 mg/kg/day for 28 days

All animal protocols were approved by the University of Colorado Committee on Animal Research, and animal care was in accordance with the National Institutes of Health guidelines for ethical animal research (NIH publication No. 80-123). Animals were housed in cages in a temperature and light-controlled environment with free access to tap water and food *ad libitum*. All drug doses were based on systematic dose finding studies during the development of the rat model, the goal of which was to achieve drug blood concentrations parallel to those of transplant patients.

Sample collection was performed as described in (13). On day 27, rats were placed in metabolic cages for 24h-urine collection. On the final day (day 28), animals were prepared for clearance measurements two hours after receiving the final drug doses as described below. Animals were sacrificed to collect both kidneys for histology and the measurement of tissue drug concentrations, and whole blood for the measurement of sirolimus/cyclosporine concentrations. Serum analysis for creatinine and blood urea nitrogen and urine analysis for creatinine was performed by the University of Colorado Hospital Laboratory (Director: Dr. R. Lepoff) using validated standard methods.

Study drugs

Oral drinking solutions of cyclosporine (Neoral, Novartis Pharma, East Hanover, NJ), sirolimus (Rapamune, Wyeth-Ayerst, Princeton, NJ) and tacrolimus capsules (Prograf, Astellas Pharma, Tokyo, Japan) were purchased from a local pharmacy. Drugs were administered by oral gavage in a constant volume according to group assignments. Sirolimus was administered in the unmodified formulation (1 mg/mL); the cyclosporine Neoral formulation was diluted in skim milk (1:10) to a final concentration of 10 mg/mL and contents of tacrolimus capsules were suspended in skim milk (1 mg/mL) prior to administration. All doses were chosen based on previous studies (14) and known to result in blood concentrations within or close to the range typically found in transplant patients. It should be noted that all drugs were administered orally and that the oral bioavailability of sirolimus and tacrolimus in rats is markedly lower than in humans.

Quantification of immunosuppressants in blood

Immunosuppressant concentrations were measured in EDTA whole blood 4 hours after the last dose on day 28 using an established, validated liquid chromatography- mass spectrometry (LC-MS) assay (15).

Glomerular filtration rates

Renal function was determined using the fluorescein isothiocyanate (FITC)-inuline method (16, 17). Two hours after the final drug dosing, rats were placed on a thermostatically controlled surgical table and anesthetized by i.p. injection of ketamine (50mg/kg)/xylazine (10mg/kg) (KetaVed/TranquiVed, Vedco, St. Joseph, MO). A 10-0 silicone catheter was inserted into the jugular vein for maintenance infusion. After injecting 2 mL of normal saline to provide sufficient intravascular volume, diluted (FITC)-inuline (Sigma, St. Louis, MO) (0.75 mg/100 mL saline) plus albumin (2.25 g/ 100 mL saline) were administered *via* perfusion pump for 2 hours at a rate of 2mL/h as previously described by Lorenz and Gruenstein (17). To monitor blood pressure throughout the experiment, a pressure transducer catheter (Millar Instruments, Houston, TX) was inserted into the carotid artery. After 1.5 hours of inuline infusion, a median laparotomy was performed, and a 10-0 silicone catheter was inserted into the left urethra. Urine was collected for 0.5 hours, and rats were sacrificed thereafter. Inuline concentration in plasma and urine was determined by fluorescence spectroscopy (Cytofluor Series 4000, Perseptive Biosystems, Framingham, MA). GFR values ($\mu\text{L}/\text{min}$) were calculated using the formula $(U \cdot V/P)$, where U equals inuline concentration in urine, V is urine output over time and P is inuline concentration in plasma. For baseline correction, blank control plasma and urine samples were enriched with different concentrations of inuline and fluorescence absorption was recorded.

Histology

For hematoxylin and eosin (H.E.) staining, kidney tissue samples were fixed in 10% buffered formaldehyde and embedded in paraffin and incubated for 5 minutes in Harris hematoxylin solution and for 60 seconds in eosin solution. Sections were washed with plain water, differentiated in 1% hydrochloric acid + 50% ethanol, and stain intensity was optimized in ammonia water. Finally, sections were rinsed in 70% ethyl alcohol and dehydrated in xylene solution.

Kidney histology was evaluated blindly. Histologies were graded based on their tubular epithelial aspects, glomerular and vascular alterations in 10 to 15 randomly selected non-overlapping fields ($\times 220$) per rat on H.E. stains according to criteria published by Lombardi *et al.* (18). Tubular injury was graded (0 to 3) based on the presence dilation/atrophy (=interstitial dilation) and presence/extent of vacuolization. Glomerular injury (GI) was graded (0 to 3) for cellularity and capillary tuft collapse (percentage of glomeruli) as a marker for glomerular ischemia and damage. Renal arterioli were evaluated with respect to the presence of hyalinosis or thrombosis (0/1).

Analysis of urine samples using $^1\text{H-NMR}$

$^1\text{H-NMR}$ analysis of urine samples was performed using a Varian INOVA NMR 600MHz spectrometer equipped with 5-mm HCN PFG probe. Rat urine (550 μL) was buffered with 73 μL 0.2M potassium phosphate buffer in D_2O prior to analysis by NMR spectroscopy. The pH was finally adjusted to 5.65–5.75 with NaOD and DCl. The external standard compound TMSP (trimethylsilyl propionic-2,2,3,3- d_4 acid dissolved in D_2O to 50mM in a thin sealed glass capillary) was inserted into the NMR tube. A standard Varian pre-saturation sequence was used to suppress water in urine. $^1\text{H-NMR}$ spectra were obtained at 600 MHz using a spectral width of 7200 Hz and 32K data arrays, and 64 scans with 90° flip angle applied

every 14.8 s. This left sufficient time for the relaxation of all proton signals integrated in this study. Data analysis was performed using MesTreC software version 4.4.1.0 (MesTreLab Research, Coruna, Spain). All spectra were normalized based on the total signal intensity. Data are presented as percent change compared to the control group.

Reagents

Urea and thiourea were purchased from Sigma-Aldrich (St. Louis, MO), CHAPS (3-[3-cholamidopropyl]-dimethylammonio]-1-propane sulfonate) and DTT (dithiothreitol) from USB (Cleveland, Ohio) and Iodoacetamide from Bio-Rad Laboratories (Hercules, CA). Protease inhibitor mix, carrier ampholytes and IPG (immobilized pH gradient) strips were obtained from GE Healthcare Bio-Sciences (Piscataway, NJ). HPLC grade water and acetonitrile came from VWR International (Westchester, PA).

Sample preparation for 2D gel electrophoresis

Freeze clamped kidneys (19) were manually homogenized using a mortar and pestle over liquid nitrogen. Approximately 90 mg of homogenized tissue was added to 1 mL of chaotropic lysis buffer (7M urea, 2M thiourea, 4% CHAPS, 50 mM DTT, 0.2% carrier ampholytes, 1% protease inhibitor mix) to extract the proteins. An electrical tissue homogenizer (PowerGen 125, Fisher Scientific) was used to further homogenize tissue in the lysis buffer. A slow setting was employed to avoid foaming and potential protein degradation. Cells in extracts were lysed on ice for 20 minutes and then centrifuged at $100,000 \times g$ for 1 h at 4°C. In order to determine protein concentrations in the supernatant, a modified Bradford Assay (Quick Start, Bio-Rad Laboratories, Hercules, CA) was carried out according to the manufacturer's protocol.

2D gel electrophoresis

Isoelectric focusing for the first dimension was carried out by rehydrating 24 cm long pH 4-7 Immobiline DryStrips (GE Healthcare, Piscataway, NJ) with 450 mL of chaotropic lysis buffer containing 1600 mg of protein. After 12 hours of active rehydration (50V, 20°C) the proteins were separated using a Protean IEF cell (Bio-Rad, (Hercules, CA)) with a voltage gradient ending at 10 kV and 70,000 volt-hours (Vh).

After the first dimension separation, strips were blotted to remove mineral oil (required to prevent strips from drying during rehydration and focusing) and stored at -80°C for at least 2 h. Prior to the second dimension separation (SDS-PAGE), thawed strips were first equilibrated with 10 mg/mL DTT in equilibration buffer (20% glycerol, 20% SDS, 1.5M Tris pH 8.8 and 6M urea), and then with 25 mg/mL iodoacetamide in equilibration buffer.

A DALT-12 chamber system with DALT 12.5 gels and the DALT buffer Kit (GE Healthcare) was used for the second dimension of separation. Equilibrated strips were cemented onto SDS-PAGE gels with 0.6% agarose. Proteins were separated by molecular weight using 60W for 30 minutes, and 180W for approximately 5 hours. Gels were maintained at 15°C during electrophoresis. Proteins were stained with Coomassie stain (Bio-Safe, Bio-Rad Laboratories, Hercules, CA) and imaged on a LabScan (GE Healthcare) at 300 dots per inch (dpi). Statistically significant changes in protein abundances were determined by IMAGE-Master platinum II software (GE Healthcare). The criterion used for the excision of 39 spots was a change in average density larger than $\pm 40\%$ of the average spot volume as compared to the control. Proteins in excised spots were identified after in-gel digestion by mass spectrometry and data base search. Hits were verified by Western-blot.

In-gel digestion

Proteins were digested in the gel spots using a modification of the methods described by Havlis et al. (20) and Hoogland et al. (21). Spots were destained with 1/1 acetonitrile and 100 mM ammonium bicarbonate, contracted with 100% acetonitrile and vacuum dried. Spots were rehydrated with 25 ng/mL trypsin and incubated for 20 min at room temperature. Excess liquid was removed and 50 mM ammonium bicarbonate (sufficient volume to cover the gel pieces) added prior to overnight incubation at 37°C. The supernatants were collected and pooled with 2 additional extracts using 1% formic acid (aqueous) with 30% acetonitrile. Pooled extracts were vacuum-concentrated to approximately 10 μ L and stored at -80°C until used.

LC-MS/MS analysis of trypsin digests

Approximately 30% of the in-gel digested sample was analyzed by reverse phase nanospray LC-MS/MS (Agilent 1100 HPLC, 75 mm \cdot 15 cm Zorbax 300 SB C18 column, Agilent Technologies, Santa Clara, CA). Peptides were eluted into the mass spectrometer using a gradient 0.1% formic acid (mobile phase A) and 90% acetonitrile and 10% 0.1% formic acid (mobile phase B) at a flow rate of 300 nL/min. The following gradient was run: 3% to 8% mobile phase B during the first minute, and then 8% to 45% over 85 min. Finally, mobile phase B was increased to 90% within 5 min and kept constant for the subsequent 10 min. Thereafter, the column was re-equilibrated to the starting conditions. Spectra were collected over an m/z range of 350–2200 Da (Agilent LC/MSD Trap XCT Plus, Agilent Technologies, Santa Clara, CA). Three MS/MS spectra were collected for the three most abundant m/z values. The masses were then excluded from analysis for 1 min and the next three most abundant m/z values were selected for fragmentation.

Protein identification using database searching

Proteins were identified by searching the NCBIInr and SwissProt databases using both Mascot (Matrix Science, Boston, MA, version 2.2.) and Spectrum Mill (Agilent Technologies, Palo Alto, CA, version 3.02) software. Using Mascot, compound lists of the resulting spectra were generated using an intensity threshold of 10,000 and a minimum of 0.2% relative abundance with grouping within 5 scans. The compound lists were exported as Mascot generic format (mgf) files and searched against the National Center for Biotechnology Information nonredundant (NCBIInr) database using a taxonomy filter for rodents. The following parameters were used for the database search: monoisotopic mass, peptide mass tolerance of 2.4 Da, fragment ion mass tolerance of 0.7 Da, tryptic peptides only allowing for 2 missed cleavages, and carbamidomethylation of cysteine as a fixed modification. Similar parameters were used for the Spectrum Mill search. Spectrum Mill protein scores above 13 with peptide scores above 10 and scored percent intensity (SPI) of 70%, were used as a cutoff for initial hit validation.

Western blot analysis

Western blot analysis was carried out to validate protein identification by data base search as described above and to confirm semi-quantitative differences in protein expression. Aliquots of frozen extracts were thawed and loaded onto a 10% polyacrylamide gel (4% stacking buffer). Proteins were separated using a Thermo EC 135-90 (Thermo LabSystems, Waltham, MA) operating for approximately 2 h at 60mA and then transferred (300 mA, 2h) from the gel to an Immobilon-P membrane.

Membranes were incubated with the primary antibody at 4°C overnight, after blocking with 5% milk in PBS Tween buffer for 10 min. Antibodies used in this study included: calbindin (rabbit anti-rat, Chemicon International, Temecula, CA), regucalcin (mouse anti-rat, Cell

Sciences, Canton, NA), NADH- ubiquinone oxidoreductase subunit 10 (chicken anti-human, GenWay, San Diego, CA), and β -actin (mouse anti-rat, Sigma Aldrich, St Louis, MO). After membranes were washed three times, the secondary antibody was applied for 4 h at room temperature. Membranes were subsequently treated with Pierce SuperSignal West Pico Solution (Pierce, Rockford, IL) following the manufacturer's protocol. A UVP BioImaging Systems UV detector (BioImaging Systems, Upland, CA) was used to detect the horseradish peroxidase reaction on the membrane. Densitometry data were normalized based on the amount of β -actin in each sample.

Statistical analysis

All numerical data are presented as means \pm standard deviations. One-way analysis of variance (ANOVA) followed by the least significant difference (LSD) method was used to determine group differences. Additionally group comparison was performed by post-hoc analysis (Holm-Sidak or Tukey method). The significance level was set at $p < 0.05$ for all tests. SigmaPlot (version 9.01) was used for graphic data analysis and SPSS (version 17.0., SPSS Inc., Chicago, IL) for statistics.

Results

Blood concentrations of immunosuppressants and kidney function markers

The concentrations of tacrolimus, cyclosporine and sirolimus in whole blood 4 hours after the last dose on day 28 are listed in Table 1. Only after day 28 of cyclosporine and cyclosporine + sirolimus treatment were creatinine concentrations in serum higher than in the controls (Table 1). At the doses tested and after 28 days of treatment, the glomerular filtration rates were lower in all groups treated with immunosuppressants both alone and in combination. Treatment with cyclosporine and cyclosporine + sirolimus had the most negative effects on glomerular filtration (Table 1). The glomerular filtration rates were ranked as follows:

Control > sirolimus = tacrolimus = tacrolimus + sirolimus > cyclosporine > cyclosporine + sirolimus.

Histology

After 28 days of treatment, none of the treatment groups showed morphological glomerular or vascular changes in comparison to control animals (score 0 for all groups). However, significant changes were observed in terms of tubular morphology. Treatment with cyclosporine (Fig. 1E) led to macro- and microvesicular tubular epithelial vacuolization (average score: 2.5 out of 3), and slight epithelial atrophy (average score: 0.5 out of 3) when compared to controls. These changes became more significant when sirolimus was added to the cyclosporine treatment protocol (Figure 1F): score for tubular epithelial vacuolization: 2.0 out of 3, score for epithelial atrophy and luminal dilation: 3.0 out of 3. The other kidney areas appeared normal, confirming that cyclosporine alone or in combination with sirolimus rather specifically target the tubuli (13).

Although usually not considered nephrotoxic when administered alone, treatment with sirolimus (Fig. 1B) also led to marked atrophy of the tubular epithelial cells with concomitant luminal dilation (average score: 2.0/ 3). Finally, kidneys from rats treated with 1 mg/kg/d tacrolimus (Fig. 1C) as well as with tacrolimus and sirolimus in combination (Fig 1D), did not display any significant differences when compared to controls (Fig. 1A). The only minor change was mild vacuolization of tubular cells (average score 1.0 out of 3). This

characteristic accumulation of cytoplasmatic vesicles with exposure to calcineurin inhibitors has been referred to as “blebs” (22).

Metabolic profiles in urine

As per our previous studies (13), treatment with the calcineurin inhibitors cyclosporine, tacrolimus and sirolimus alone or in combination led to significant changes in urine metabolite patterns (Figure 2 and Figure 3). These changes corresponded to those previously described for S3 tubular damage (23) and also matched the histology results described above. Again, sirolimus alone significantly affected urine metabolite patterns after 28 days of treatment (Figure 2). At the doses tested, tacrolimus and the combination of tacrolimus + sirolimus resulted in urine metabolite pattern changes that were less pronounced than those observed after treatment with cyclosporine and cyclosporine + sirolimus. This indicates less of an effect on tubulus cells than cyclosporine alone or in combination with sirolimus and was most obvious when comparing glucose concentrations in urine (Figure 2). When combined with calcineurin inhibitors, especially with cyclosporine, sirolimus enhanced the effects of calcineurin inhibitors on urine metabolite pattern changes. The effects of immunosuppressants and their combinations on urine metabolite patterns at the doses tested were ranked as follows:

$$\text{Control} < \text{sirolimus} = \text{tacrolimus} = \text{tacrolimus} + \text{sirolimus} < \text{cyclosporine} < \text{cyclosporine} + \text{sirolimus}.$$

The treatment with tacrolimus and combination of tacrolimus with sirolimus revealed several specific changes that were not observed after cyclosporine treatment. The urinary concentration of N-methyl nicotinamide increased to a statistically significant level ($p < 0.01$) from 0.32 ± 0.14 ‰ of total integral in the control group to 0.80 ± 0.06 ‰ after tacrolimus treatment and 0.65 ± 0.06 ‰ after tacrolimus + sirolimus. The combination of tacrolimus with sirolimus also resulted in a 8-fold increase in the concentration of TMAO from 28 ± 8 ‰ of total integral in the controls to 218 ± 8 ‰ of total integral in the combination treatment.

Proteome analysis

Gel image analysis was carried out using the ImageMaster 2D Platinum II software version 5.0. The spot auto-detect function was used for all group comparisons using the same parameters. Groups were matched automatically and corrected manually when necessary. Differences in protein expression were identified using the relative volume (% Vol) option offered by the software. This option allows a spot normalization to make data independent of experimental variations between gels caused by differences in loading or staining. Relative volume was calculated as follows:

$$\% \text{ Vol} = \frac{\text{Vol}}{\sum_{s=1}^n \text{Vol}_s} \times 100 \quad \text{with Vol}_s: \text{volume of spot } s \text{ in a gel containing } n \text{ spots.}$$

Raw spot values were normalized using the software's ratio option according to the following equation:

$$\text{Ratio} = \frac{\text{spot values}_s}{\text{central tendency}} \quad \text{with central tendency: mean of spot } s.$$

Approximately 1500 proteins per gel were detected depending on the threshold used. The spots of 24 gels (6 groups, n = 4 each group) were grouped resulting in 800 groups of protein spots. To qualify as a group, specific spots had to appear on 23 out of 24 gels. This requirement kept the false assignments of spots to a minimum.

Seventy-five significant protein spot changes were detected, from which 37 protein spots were cut from the membrane based on a threshold change in average spot volume larger than $\pm 40\%$ (and significance levels of $p < 0.05$; control vs. treated groups). Seven of these spots represented the major urinary protein (alpha-2 microglobulin) and three other proteins were each represented by two spots. Protein hits are summarized in Table 2. The kidney proteins affected by treatment with immunosuppressants and their combinations at the doses tested for 28 days could be summarized into the following groups based on function: cytoskeletal proteins, proteins involved in calcium homeostasis, proteins involved in mitochondrial function, and proteins involved in cell metabolism.

Cytoskeletal proteins: vimentin, caldesmon, actin binding protein 1 (ABP1), actin related protein 3 ARP3, and plastin 3T isoform

The concentration of the cytoskeletal or the cytoskeleton related proteins vimentin, caldesmon, actin binding protein 1 (ABP1), actin related protein 3 (ARP3) and plastin 3T isoform increased up to 1.6- to 2.5-fold (Table 2 and Figure 4) with immunosuppressant treatment. These proteins are mainly expressed in endothelial cells, smooth muscle cells (mesangial cells) and fibroblasts. The exception is plastin 3T, which is present in all cell types.

Proteins involved in calcium homeostasis: regucalcin and calbindin

Regucalcin (or senescence marker protein 30) plays a pivotal role in maintaining the intracellular Ca^{2+} homeostasis due to activation of Ca^{2+} pumps in the plasma membrane (basolateral membrane), microsomes (endoplasmic reticulum) and mitochondria of many cell types (24). There was an observed decrease in regucalcin protein concentrations after treatment with cyclosporine, sirolimus or their combination (Table 2). A second signal at -0.1 pH units with the same mass and the same protein ID as the regucalcin spot was also detected (Figure 5). The volume of this spot increased especially following treatment with sirolimus, cyclosporine and their combination. It appeared to have an inverse correlation with the volume of the other regucalcin spot. Surprisingly, sirolimus displayed a very similar effect on this protein as cyclosporine, whereas tacrolimus and the combination of tacrolimus with sirolimus did not affect regucalcin expression.

Calbindin plays a crucial role for Ca^{2+} transport in kidney tubulus cells (25). This 28kDa calcium binding protein (six Ca^{2+} ions per protein) was significantly down-regulated after treatment with the calcineurin inhibitors cyclosporine and tacrolimus. This was shown using 2D gel electrophoresis (Table 2) and Western blot analysis (Figure 6). It is interesting to observe that calbindin expression was not reduced by sirolimus or the combination of tacrolimus and sirolimus, but was reduced when sirolimus was co-administered with cyclosporine.

Mitochondrial dysfunction: NADH-ubiquinone oxidoreductase (NADH-UO)

The concentration of one modification of the mitochondrial enzyme NADH-UO, which participates in complex I of the respiratory chain, underwent a significant reduction when rats were treated with sirolimus or cyclosporine alone and when both immunosuppressants were co-administered. As shown in Figure 7, the protein spot representing NADH-UO subunit 10 on the 2D gels is reduced following immunosuppressant treatment. This was confirmed by Western blot and NADH-UO spot on the 2D-gels correlating with the lowest

band observed in the Western blot analysis (Figure 7, bottom). In the case of sirolimus and cyclosporine+sirolimus treatments reduced expression of NADH-UO oxidoreductase expression corresponded well with the reduction of TCA cycle metabolite concentrations in urine (Table 3A).

Cell metabolism: arginine:glycine-amidino transferase (AGAT) and kidney aminoacylase (KA), pyruvate kinase and fructose-1,6-bisphosphatase (F-1,6-BP)

Arginine:glycine-amidino transferase (AGAT) catalyses the first reaction in creatine biosynthesis, transferring the amidino group from arginine to glycine to yield ornithine and guanidinoacetic acid. The guanidinoacetate that is produced in the kidney can enter circulation for transport to the liver, where it is a substrate for S-adenosyl-L-methionine: guanidino acetate N-methyl transferase that forms creatine (26). AGAT tissue concentration was 4-fold increased after sirolimus treatment and treatment with tacrolimus + sirolimus.

Expression of pyruvate kinase (8), an enzyme involved in the regulation of the glycolytical activity, increased in all treatment groups, and especially in the cyclosporine + sirolimus combination (more than 2-fold, Table 3A). This corresponds to our previous findings, where we have reported that rats treated with cyclosporine and its combination with sirolimus exhibit an increased glycolysis rate and lactate production (13).

Kidney aminoacylase I (KA-1) is an enzyme which catalyzes the reaction of hippuric acid to benzoic acid and glycine (27). The decrease in hippuric acid concentrations in urine correlated with the increase in kidney amino acylase enzyme in all treated groups (Table 3B).

Fructose-1,6-bisphosphatase is the rate-regulating enzyme for gluconeogenesis (28). Fructose-1,6-bisphosphatase expression was increased in the presence of cyclosporine alone and in combination with sirolimus, while tacrolimus, sirolimus and the combination of tacrolimus and sirolimus did not have any effect (Table 2).

Discussion

Several potential protein biomarkers for the renal damage caused by the immunosuppressive drugs could be identified in this study. These include structural proteins such as caldesmon and vimentin, proteins involved in calcium homeostasis such as regucalcin and calbindin and metabolizing enzymes such as pyruvate kinase and NADH-ubiquinone oxidoreductase. The results of the present study further showed that immunosuppressant-induced changes in protein expression in the kidney explain several of the metabolite pattern changes in urine and provide further insight into the toxicity mechanisms.

To ensure that our immunosuppressant doses had yielded adequate systemic exposure, blood concentrations 4 hours after the last dose on day 28 were measured using a specific and validated HPLC-MS assay (15). The cyclosporine and sirolimus concentrations in blood were as expected based on previous studies (13) and within the blood concentration range in transplant patients. With 3.0 ± 2.5 ng/mL after 4 hours, the tacrolimus doses resulted in blood concentrations on the lower end of the target concentration range in patients. Maintenance trough blood concentrations measured 12 hours after the last tacrolimus dose typically range from 3–10 ng/mL (29). This needs to be taken into account when comparing results between cyclosporine and tacrolimus alone or in combination with sirolimus. However, it is reasonable to expect that this will impact the extent of the changes and not mechanistic differences such as which proteins or metabolites are affected.

Our results confirmed our previous observation that the immunosuppressants specifically target the tubulus, and that at the doses tested, tacrolimus affects the kidney to a lesser extent than cyclosporine alone or in combination with sirolimus. The histology results matched the urine metabolite patterns by showing changes known to be associated with S3 tubular damage (13, 23, 30).

Analysis of the effects of immunosuppressants on protein expression in the kidney provided further insight into their mechanisms of action and toxicity induction.

Cytoskeletal proteins

Treatment with immunosuppressants increased the kidney tissue concentrations of several cytoskeletal proteins. Makino et al. showed that the expression of the contractile-associated protein caldesmon may serve as an early marker for the development of glomerulosclerosis (31). The fact that cyclosporine causes glomerulosclerosis is well described in the literature (32). It can be hypothesized that caldesmon is a potential marker for the glomerulosclerosis caused by cyclosporine. Vimentin is an intermediate filament protein that, although absent in normal adult tubular cells, is a known marker of cell damage when present in tubulus cells (33). Increased vimentin levels in kidney tissue are therefore a potential indicator for tubular injury. In our study, the increase of vimentin expression was associated with the extent of tubular damage. Thus, the highest vimentin concentrations (2.5-fold increase) were found when sirolimus and cyclosporine were co-administered. However, because 2D-gel analysis was based on homogenates of the whole kidney, the possibility that other cell types may have contributed cannot be excluded.

Actin binding protein 1 (ABP1 or drebrin) and actin-related protein 3 (ARP3) are both present in mesangial cells (34). Although the mechanisms are not fully understood, both proteins are involved in actin mobility. Kessels *et al.* (35) showed, that growth factors can lead to accumulation of ABP1 in actin-rich filaments which is accompanied by high ARP2/3 complex concentrations with actin bundling activity. Plastins, which were also overexpressed after cyclosporine treatment, appear to play a role in actin-binding. While actin-bundling activity by mammalian plastins is well established, additional evidence for actin filament stabilization also exists. The over-expression of ABP1, ARP1, plastins and caldesmon in kidney tissue after cyclosporine treatment may also indicate changes in the mesangial cells. Acute cyclosporine treatment was shown to induce contraction in smooth muscle and mesangial cells *in vitro* (36).

Calcium homeostasis

Regucalcin (or senescence marker protein 30) expression was affected by cyclosporine, sirolimus and cyclosporine + sirolimus, but not tacrolimus. It plays a pivotal role in the maintenance of the intracellular Ca^{2+} homeostasis due to activation of Ca^{2+} pumps in the plasma membrane (basolateral membrane), microsomes (endoplasmatic reticulum) and mitochondria of many cell types (24). It has been shown that cyclosporine reduces the concentration of regucalcin (37). This verifies the observation made in our study. The effect of sirolimus on regucalcin alone and in combination with cyclosporine has not yet been described. Regucalcin regulates many intracellular calcium-dependent pathways. It increases the activities of plasma membrane $\text{Ca}^{2+}/\text{Mg}^{2+}$ -ATPase (pumping Ca^{2+} out of the cell) and the mitochondrial Ca^{2+} -ATPase (pumping Ca^{2+} into the mitochondria) (38) as well as cytosolic $[\text{Ca}^{2+}]_i$; and it causes mitochondrial $[\text{Ca}^{2+}]_m$ overload *in vitro* (39, 40). Under physiological conditions Ca^{2+} /calmodulin stimulates the transcription of the regucalcin gene *via* Ca^{2+} /calmodulin-dependent protein kinase (CaM kinase) pathway. On the other hand, regucalcin is known to antagonize the effects of Ca^{2+} /Calmodulin (24). A lower transcription rate of regucalcin indicates less CaM kinase activity. Further investigation will

be required to determine: how cyclosporine and sirolimus alone and in combination decrease regucalcin, how this relates to the other protein that has a regucalcin structure but is located at a different pI, and why tacrolimus does not affect regucalcin.

Calbindin kidney tissue concentrations were not reduced by sirolimus, but by the calcineurin inhibitors. It plays several roles in the tubulus cells. One such role entails the reabsorption of Ca^{2+} from urine. As demonstrated previously, cyclosporine increases urinary calcium concentrations. Our results may explain these findings since decreased calbindin levels lead to a decrease in reabsorption and a subsequent increase in Ca^{2+} levels in urine. Calbindin also acts as an intracellular calcium buffer. Though it has not yet been shown that co-administration of cyclosporine and sirolimus have an additive effect on calbindin, it is possible to speculate its involvement in the tubular calcification and increased urinary calcium levels caused by cyclosporine (41).

Mitochondrial dysfunction/ metabolizing enzymes

Pyruvate kinase, a rate-regulating glycolytical enzyme, can be over-expressed in anaerobic conditions (42). The combination of cyclosporine with sirolimus resulted in a 2.2-fold increase of this enzyme. This may indicate increased glycolytic activity caused by the inhibition of the TCA cycle as previously observed in brain cells (43). A higher concentration of this enzyme results in increased formation of pyruvate that then can be transformed into lactate by lactate dehydrogenase. Higher lactate levels after cyclosporine treatment were observed in tissue and blood (43, 44). Accordingly, we detected an increase in urinary lactate levels compared to vehicle controls following treatment with cyclosporine and co-administration of cyclosporine and sirolimus.

Complex I is the rate-regulating step in the respiratory chain (45). As previously shown (43, 44) and observed in the present study (Table 2), cyclosporine reduces mitochondrial metabolism and increases mitochondrial oxygen radical concentrations. The exact cause-effect relationship that leads to the reduction in NADH-ubiquinone oxidoreductase is not yet determined.

Stead et al (26) showed that increased creatine blood levels lead to a decrease of AGAT protein as a feed back mechanism. Our data suggests that the treatment with sirolimus, but not with the calcineurin inhibitors is associated with increased urinary concentrations of creatine after 28 days of treatment. In comparison to the controls and the calcineurin inhibitor mono-treatment groups, AGAT protein expression was reduced in the kidneys of rats treated sirolimus.

Diabetes mellitus is a major complication of immunosuppressive drug regimens after transplantation based on the calcineurin inhibitors cyclosporine or tacrolimus that are known to enhance new-onset diabetes (46, 47). The liver, and to a lesser extend the kidney, are the primary organs responsible for endogenous glucose production (28). Fructose-1,6-bisphosphatase (F-1,6-BPase) is the rate-regulating enzyme for gluconeogenesis (28). Inhibition of the production of endogenous glucose by F-1,6-BPase is known to have an anti-diabetic effect (48). The observed increase in F-1,6-BPase concentrations in kidney tissue is another indicator that cyclosporine alone and in combination with sirolimus changes glucose metabolism in the kidney. Interestingly, the expression of this enzyme was not changed after treatment with tacrolimus alone or in combination with sirolimus.

Overall, the results of the present study showed agreement among immunosuppressant-induced changes of histology, kidney function parameters, kidney tissue protein expression and urine metabolite patterns and confirmed and extended our previous results (13). These indicated that cyclosporine alone or in combination with sirolimus mainly target proximal

tubulus cells in the kidney and inhibit mitochondrial oxidation leading to increased oxygen radical formation and inhibition of the TCA cycle. This results in increased uptake of TCA intermediates from urine via Na(+)/dicarboxylate transporters and increased anaerobic glycolysis. The results of the present study support and further explain (qualify) these previous findings. One of the most important results was that although, like cyclosporine, tacrolimus exposure resulted in urine metabolite pattern changes indicating that the proximal tubulus is an initial target, differences in its effects on protein patterns suggest that both calcineurin inhibitors act through different signaling pathways in inducing toxicity. The most striking difference was their effect on regucalcin concentrations in kidney tissue. The present study also provided further confirmation that in our model and at the doses tested, sirolimus--often believed to have no effect on the kidney if administered alone—does in fact cause changes in protein expression and urine metabolite patterns.,

Although the number of animals used for the proteome analysis part of this study (n=4) was relatively small, the data was consistent among the treatment groups. Confidence in the data was further strengthened by the fact that many of the proteomic changes could be confirmed by Western blot analysis and that many of the changes of enzyme protein concentrations could be linked to changes of corresponding metabolites.

Several potential protein biomarkers for the glomerular and tubular damage caused by the calcineurin inhibitors alone and in combination with sirolimus could be identified in this study. Future studies using targeted and more quantitative assays will further establish the sensitivity and specificity of these potential markers in kidney tissues and urine and will evaluate if these markers translate into transplant patients.

Acknowledgments

The study was supported by the United States National Institutes of Health (NIH), grants R01 DK065094 and P30 DK048520 (Mass Spectrometry Core).

References

1. Wong W, Venetz JP, Tolckoff-Rubin N, Pascual M. 2005 immunosuppressive strategies in kidney transplantation: which role for the calcineurin inhibitors? *Transplantation*. 2005; 80(3):289. [PubMed: 16082321]
2. Taylor AL, Watson CJ, Bradley JA. Immunosuppressive agents in solid organ transplantation: Mechanisms of action and therapeutic efficacy. *Crit Rev Oncol Hematol*. 2005; 56(1):23. [PubMed: 16039869]
3. Ojo AO, Held PJ, Port FK, et al. Chronic renal failure after transplantation of a nonrenal organ. *N Engl J Med*. 2003; 349(10):931. [PubMed: 12954741]
4. Ponticelli C, Tarantino A. Promising new agents in the prevention of transplant rejection. *Drugs R D*. 1999; 1(1):55. [PubMed: 10565988]
5. Kahan BD. The Rapamune US Study Group. Efficacy of sirolimus compared with azathioprine for reduction of acute renal allograft rejection: a randomised multicentre study. *Lancet*. 2000; 356(9225):194. [PubMed: 10963197]
6. Andoh TF, Lindsley J, Franceschini N, Bennett WM. Synergistic effects of cyclosporine and rapamycin in a chronic nephrotoxicity model. *Transplantation*. 1996; 62(3):311. [PubMed: 8779675]
7. Brook NR, Waller JR, Bicknell GR, Nicholson ML. Cyclosporine and rapamycin act in a synergistic and dose-dependent manner in a model of immunosuppressant-induced kidney damage. *Transplant Proc*. 2005; 37(2):837. [PubMed: 15848549]
8. Podder H, Stepkowski SM, Napoli KL, et al. Pharmacokinetic interactions augment toxicities of sirolimus/cyclosporine combinations. *J Am Soc Nephrol*. 2001; 12(5):1059. [PubMed: 11316866]

9. Christians U, Reisdorff N, Klawitter J, Schmitz V. Biomarkers of immunosuppressive drug toxicity. *Curr Opin Transplant.* 2005; 10(4):284.
10. Merville P. Combating chronic renal allograft dysfunction: optimal immunosuppressive regimens. *Drugs.* 2005; 65(5):615. [PubMed: 15748097]
11. Gummert JF, Ikonen T, Morris RE. Newer immunosuppressive drugs: a review. *J Am Soc Nephrol.* 1999; 10(6):1366. [PubMed: 10361877]
12. Schmitz V, Klawitter J, Bendrick-Peart J, et al. Metabolic profiles in urine reflect nephrotoxicity of sirolimus and cyclosporine following rat kidney transplantation. *Nephron Exp Nephrol.* 2009; 111(4):e80. [PubMed: 19293597]
13. Klawitter J, Bendrick-Peart J, Rudolph B, et al. Urine metabolites reflect time-dependent effects of cyclosporine and sirolimus on rat kidney function. *Chem Res Toxicol.* 2009; 22(1):118. [PubMed: 19099400]
14. Christians U, Schmitz V, Schoning W, et al. Toxicodynamic therapeutic drug monitoring of immunosuppressants: promises, reality, and challenges. *Ther Drug Monit.* 2008; 30(2):151. [PubMed: 18367974]
15. Christians U, Jacobsen W, Serkova N, et al. Automated, fast and sensitive quantification of drugs in blood by liquid chromatography-mass spectrometry with on-line extraction: immunosuppressants. *J Chromatogr B Biomed Sci Appl.* 2000; 748(1):41. [PubMed: 11092585]
16. Fleck C. Determination of the glomerular filtration rate (GFR): methodological problems, age-dependence, consequences of various surgical interventions, and the influence of different drugs and toxic substances. *Physiol Res.* 1999; 48(4):267. [PubMed: 10638678]
17. Lorenz JN, Gruenstein E. A simple, nonradioactive method for evaluating single-nephron filtration rate using FITC-inulin. *Am J Physiol.* 1999; 276(1 Pt 2):F172. [PubMed: 9887093]
18. Lombardi D, Gordon KL, Polinsky P, Suga S, Schwartz SM, Johnson RJ. Salt-sensitive hypertension develops after short-term exposure to Angiotensin II. *Hypertension.* 1999; 33(4):1013. [PubMed: 10205240]
19. Wollenberger A, Ristau O, Schoffa G. A simple technic for extremely rapid freezing of large pieces of tissue. *Pflugers Arch Gesamte Physiol Menschen Tiere.* 1960; 270:399.
20. Havlis J, Thomas H, Sebela M, Shevchenko A. Fast-response proteomics by accelerated in-gel digestion of proteins. *Anal Chem.* 2003; 75(6):1300. [PubMed: 12659189]
21. Hoogland C, Walther D, Palagi PM, et al. A suite of tools to analyse and publish 2-DE data. *Proteomics.* 2008; 8(23-24):4907. [PubMed: 19072735]
22. Torhorst J, de Rougemont D, Brunner FP, Thiel G. Morphology of the renal medulla in ischemic acute renal failure in the rat. *Nephron.* 1982; 31(4):296. [PubMed: 7177265]
23. Bairaktari E, Katopodis K, Siamopoulos KC, Tsolas O. Paraquat-induced renal injury studied by ¹H nuclear magnetic resonance spectroscopy of urine. *Clin Chem.* 1998; 44(6 Pt 1):1256. [PubMed: 9625050]
24. Yamaguchi M. Role of regucalcin in maintaining cell homeostasis and function (review). *Int J Mol Med.* 2005; 15(3):371. [PubMed: 15702226]
25. Wu MJ, Lai LW, Lien YH. Effect of calbindin-D28K on cyclosporine toxicity in cultured renal proximal tubular cells. *J Cell Physiol.* 2004; 200(3):395. [PubMed: 15254967]
26. Stead LM, Au KP, Jacobs RL, Brosnan ME, Brosnan JT. Methylation demand and homocysteine metabolism: effects of dietary provision of creatine and guanidinoacetate. *Am J Physiol Endocrinol Metab.* 2001; 281(5):E1095. [PubMed: 11595668]
27. Heese D, Rohm KH. Reactivities of sulfhydryl groups in native and metal-free aminoacylase I. *Biol Chem Hoppe Seyler.* 1989; 370(6):607. [PubMed: 2775487]
28. Erion MD, van Poelje PD, Dang Q, et al. MB06322 (CS-917): A potent and selective inhibitor of fructose 1,6-bisphosphatase for controlling gluconeogenesis in type 2 diabetes. *Proc Natl Acad Sci U S A.* 2005; 102(22):7970. [PubMed: 15911772]
29. Wallemaq P, Armstrong VW, Brunet M, et al. Opportunities to optimize tacrolimus therapy in solid organ transplantation: report of the European consensus conference. *Ther Drug Monit.* 2009; 31(2):139. [PubMed: 19177031]
30. Shockcor JP, Holmes E. Metabonomic applications in toxicity screening and disease diagnosis. *Curr Top Med Chem.* 2002; 2(1):35. [PubMed: 11899064]

31. Makino H, Kashihara N, Sugiyama H, et al. Phenotypic changes of the mesangium in diabetic nephropathy. *J Diabetes Complications*. 1995; 9(4):282. [PubMed: 8573747]
32. Alonso EM. Long-term renal function in pediatric liver and heart recipients. *Pediatr Transplant*. 2004; 8(4):381. [PubMed: 15265166]
33. Ofstad J, Iversen BM. Glomerular and tubular damage in normotensive and hypertensive rats. *Am J Physiol Renal Physiol*. 2005; 288(4):F665. [PubMed: 15536168]
34. Peitsch WK, Hofmann I, Endlich N, et al. Cell biological and biochemical characterization of drebrin complexes in mesangial cells and podocytes of renal glomeruli. *J Am Soc Nephrol*. 2003; 14(6):1452. [PubMed: 12761245]
35. Kessels MM, Engqvist-Goldstein AE, Drubin DG. Association of mouse actin-binding protein 1 (mAbp1/SH3P7), an Src kinase target, with dynamic regions of the cortical actin cytoskeleton in response to Rac1 activation. *Mol Biol Cell*. 2000; 11(1):393. [PubMed: 10637315]
36. Dubus I, Sena S, Labouyrie JP, Bonnet J, Combe C. In vitro prevention of cyclosporin-induced cell contraction by mycophenolic acid. *Life Sci*. 2005; 77(26):3366. [PubMed: 15978635]
37. Aicher L, Wahl D, Arce A, Grenet O, Steiner S. New insights into cyclosporine A nephrotoxicity by proteome analysis. *Electrophoresis*. 1998; 19(11):1998. [PubMed: 9740060]
38. Mori S, Yamaguchi M. Calcium-binding protein regucalcin stimulates the uptake of Ca²⁺ by rat liver mitochondria. *Chem Pharm Bull (Tokyo)*. 1991; 39(1):224. [PubMed: 2049806]
39. Carvalho da Costa M, de Castro I, Neto AL, Ferreira AT, Burdmann EA, Yu L. Cyclosporin A tubular effects contribute to nephrotoxicity: role for Ca²⁺ and Mg²⁺ ions. *Nephrol Dial Transplant*. 2003; 18(11):2262. [PubMed: 14551352]
40. Jiang T, Acosta D Jr. Mitochondrial Ca²⁺ overload in primary cultures of rat renal cortical epithelial cells by cytotoxic concentrations of cyclosporine: a digitized fluorescence imaging study. *Toxicology*. 1995; 95(1–3):155. [PubMed: 7825182]
41. Aicher L, Meier G, Norcross AJ, et al. Decrease in kidney calbindin-D 28kDa as a possible mechanism mediating cyclosporine A- and FK-506-induced calciuria and tubular mineralization. *Biochem Pharmacol*. 1997; 53(5):723. [PubMed: 9113092]
42. Yamada K, Noguchi T. Regulation of pyruvate kinase M gene expression. *Biochem Biophys Res Commun*. 1999; 256(2):257. [PubMed: 10079172]
43. Serkova N, Jacobsen W, Niemann CU, et al. Sirolimus, but not the structurally related RAD (everolimus), enhances the negative effects of cyclosporine on mitochondrial metabolism in the rat brain. *Br J Pharmacol*. 2001; 133(6):875. [PubMed: 11454661]
44. Serkova N, Klawitter J, Niemann CU. Organ-specific response to inhibition of mitochondrial metabolism by cyclosporine in the rat. *Transpl Int*. 2003; 16(10):748. [PubMed: 12827232]
45. Sharma LK, Lu J, Bai Y. Mitochondrial respiratory complex I: structure, function and implication in human diseases. *Curr Med Chem*. 2009; 16(10):1266. [PubMed: 19355884]
46. Smith RM. CMV prophylaxis: a useful step towards prevention of post-transplant diabetes? *Diabetologia*. 2004; 47(9):1473. [PubMed: 15338130]
47. Kari JA, Trompeter RS. What is the calcineurin inhibitor of choice for pediatric renal transplantation? *Pediatr Transplant*. 2004; 8(5):437. [PubMed: 15367278]
48. McCormack JG, Westergaard N, Kristiansen M, Brand CL, Lau J. Pharmacological approaches to inhibit endogenous glucose production as a means of anti-diabetic therapy. *Curr Pharm Des*. 2001; 7(14):1451. [PubMed: 11529255]
49. Lungkaphin A, Lewchalermwongse B, Chatsudthipong V. Relative contribution of OAT1 and OAT3 transport activities in isolated perfused rabbit renal proximal tubules. *Biochim Biophys Acta*. 2006; 1758(6):789. [PubMed: 16815243]

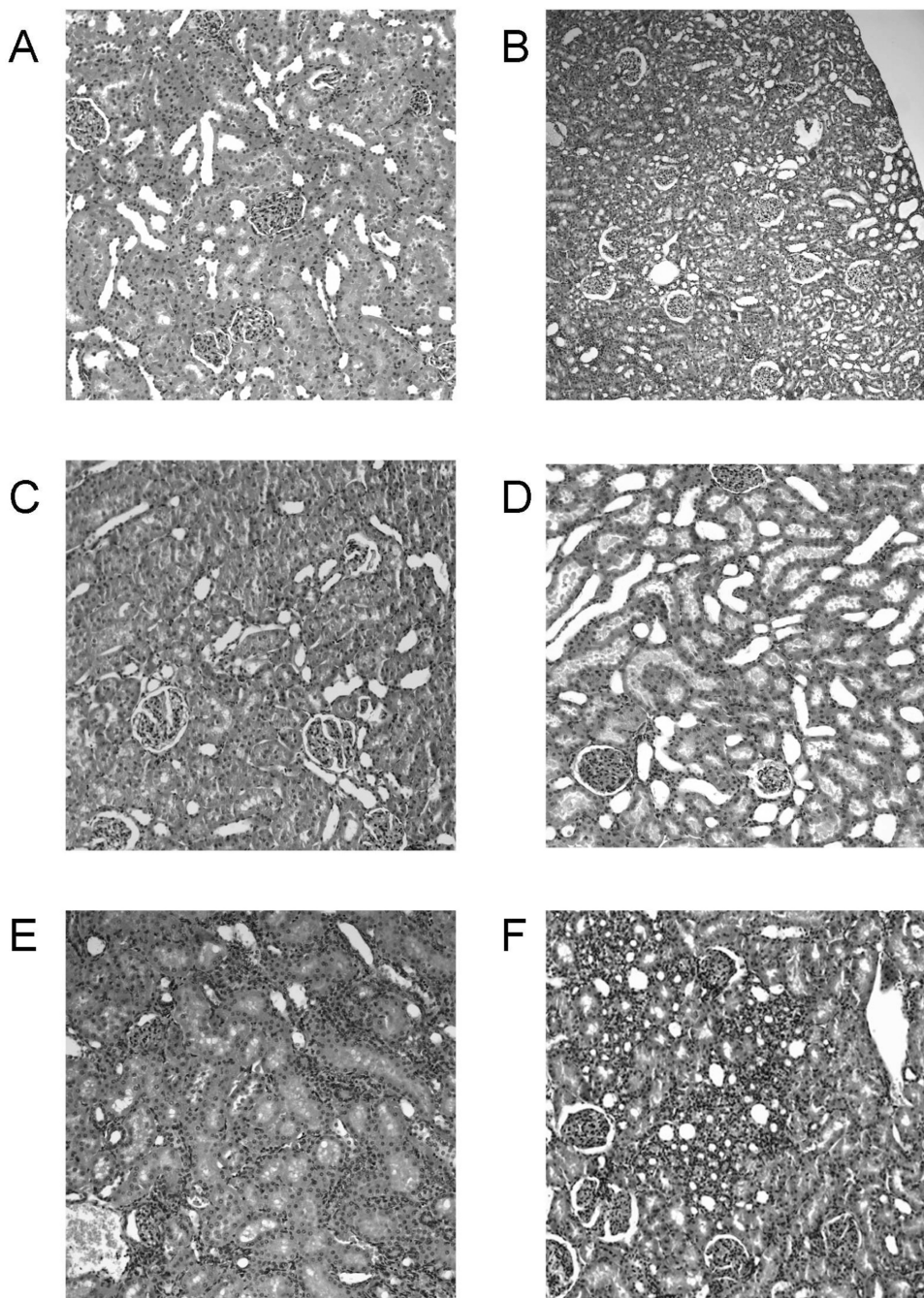


Figure 1. Representative histology (HE stain) of kidney tissues from the different treatment groups

The total number of tissue samples evaluated was n=6/ treatment group. All figures: $\times 440$ magnification, except for B: 7220 magnification to better illustrate the overall appearance of tubular dilation. None of the groups showed structural changes of either glomerular or vascular aspects and changes caused by the immunosuppressants alone and in combination at the doses tested were mostly focused on the tubuli.

- A) kidney sample from vehicle-treated control
 B) 1 mg/kg/d sirolimus: minor tubular epithelial atrophy and luminal dilation,
 C) 1 mg/kg/d tacrolimus: no differences compared to vehicle-treated controls,

D) 1 mg/kg/d tacrolimus+ 1 mg/kg/day sirolimus: tubular dilation similar to B), in addition dilated tubular lumen filled with cytoplasmic vesicles (blebs) leading to luminal narrowing in some parts.

E) 10 mg/kg/d cyclosporine: macro- and microvesicular intracellular vacuolization of the tubular epithelial cells combined with marked shrinking (atrophy) and luminal dilation of the proximal and distal tubular cytoplasm,

F) 10 mg/kg/d cyclosporine+ 1 mg/kg/day sirolimus: same effects as described for E) but more progressed damage. Areas adjacent to the tubuli appeared normal leading to an overall inhomogeneous appearance.

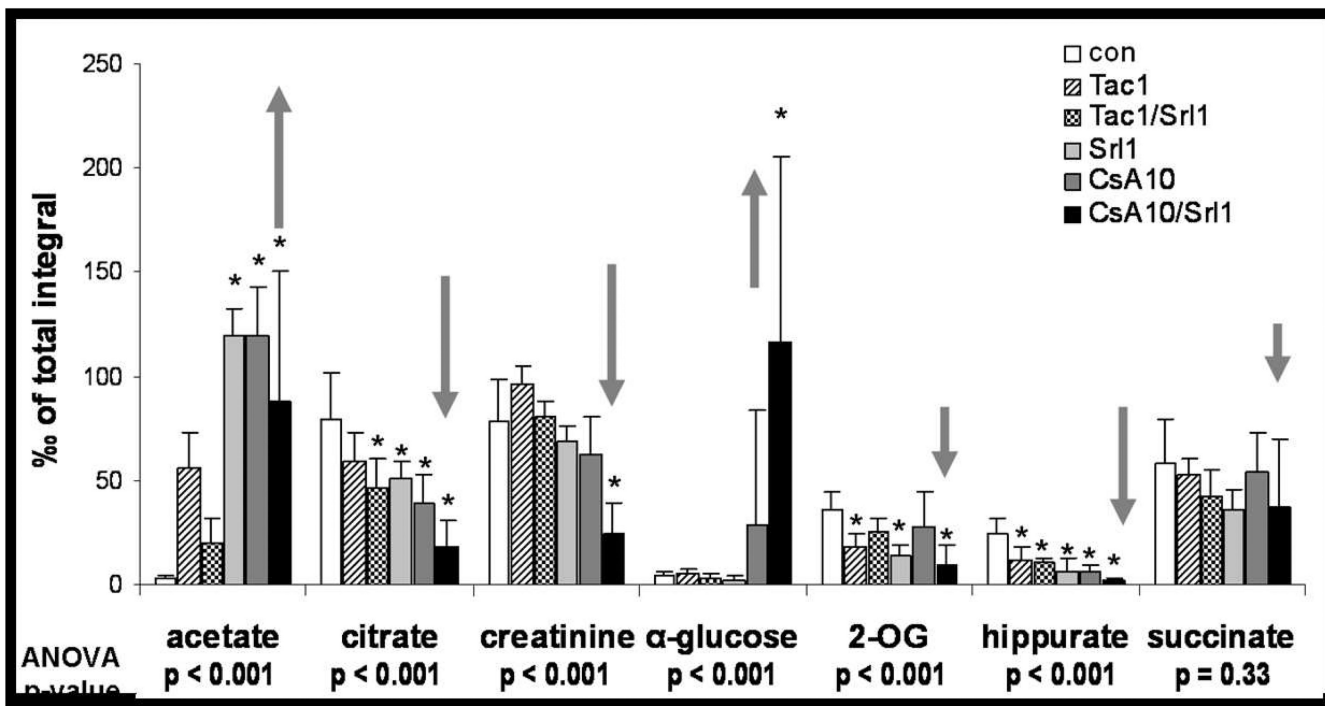


Figure 2. Changes in urinary metabolite patterns after 28 days as assessed using ^1H NMR spectroscopy

Metabolites known to be associated with proximal tubulus injury (21) are shown.

Significance level: * $p < 0.05$ (Tukey test pairwise comparison to controls). All values are normalized based on the total integral to compensate for differences in urine concentrations and are presented at means + standard deviations ($n=6$). The arrows show the expected direction of changes indicating tubular damage (21,30). Abbreviations: CsA10: 10 mg/kg/d cyclosporine, CsA10+Srl1: 10 mg/kg/d cyclosporine+ 1 mg/kg/d sirolimus, Srl1: 1 mg/kg/d sirolimus, Tac1: 1 mg/kg/d tacrolimus, Tac1+Srl1: 1 mg/kg/d tacrolimus + 1 mg/kg/d sirolimus.

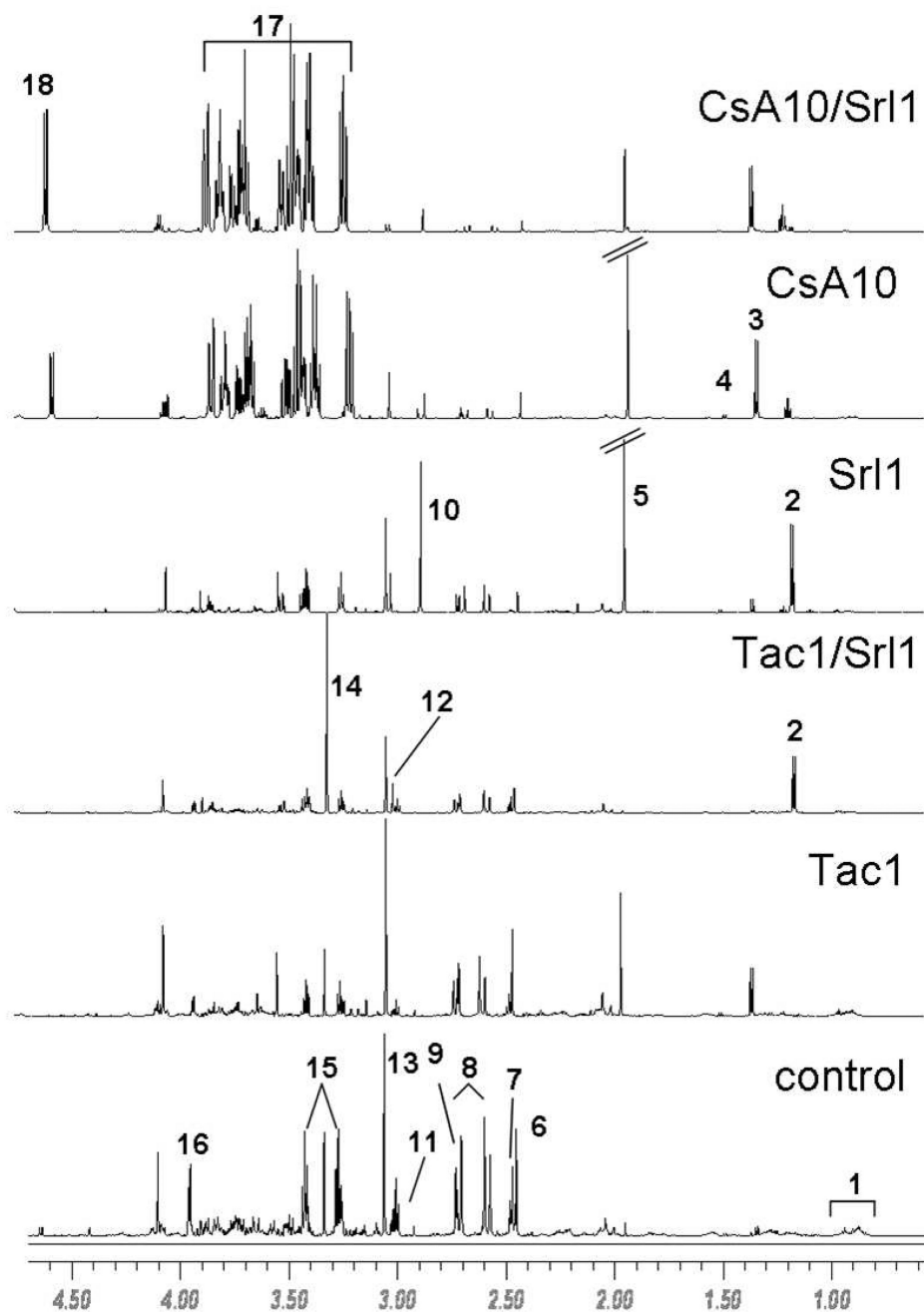


Figure 3. Representative ^1H -NMR spectra of urine samples

The total number of urine samples evaluated for each group was $n=6$. Signal assignments: 1 valine leucine isoleucine 2 sirolimus drug vehicle compounds, 3 lactate, 4 alanine, 5 acetate, 6 succinate, 7 2-oxoglutarate, 7 citrate, 8 dimethylamine, 10 trimethylamine, 11 dimethyl glycine, 12 creatine, 13 creatinine, 14 trimethylamine oxide, 15 taurine, 16 hippurate, 17 glucose, 18 α -glucose. Abbreviations: CsA10: 10 mg/kg/d cyclosporine, CsA10/Srl1: 10 mg/kg/d cyclosporine+ 1 mg/kg/d sirolimus, Srl1: 1 mg/kg/d sirolimus, Tac1: 1 mg/kg/d tacrolimus, Tac1/Srl1: 1 mg/kg/d tacrolimus + 1 mg/kg/d sirolimus.

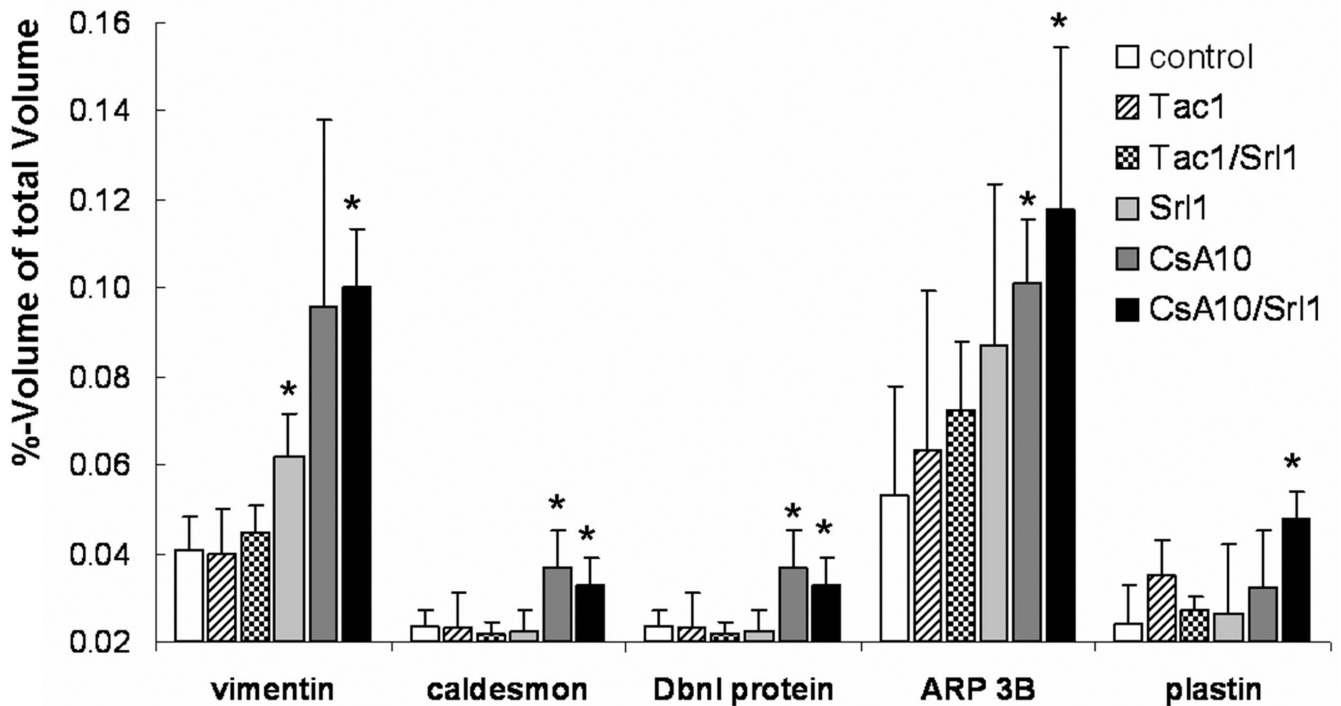


Figure 4. Changes in concentration of proteins that are involved in structural integrity and contractile processes based on the analysis of 2D-gels

Significance levels: *: $p < 0.05$ (Tukey test pairwise comparison to controls). All values are means \pm standard deviations ($n=4$). Abbreviations: CsA10: 10 mg/kg/d cyclosporine, CsA10+Srl1: 10 mg/kg/d cyclosporine+ 1 mg/kg/d sirolimus, Srl1: 1 mg/kg/d sirolimus, Tac1: 1 mg/kg/d tacrolimus, Tac1+Srl1: 1 mg/kg/d tacrolimus + 1 mg/kg/d sirolimus.

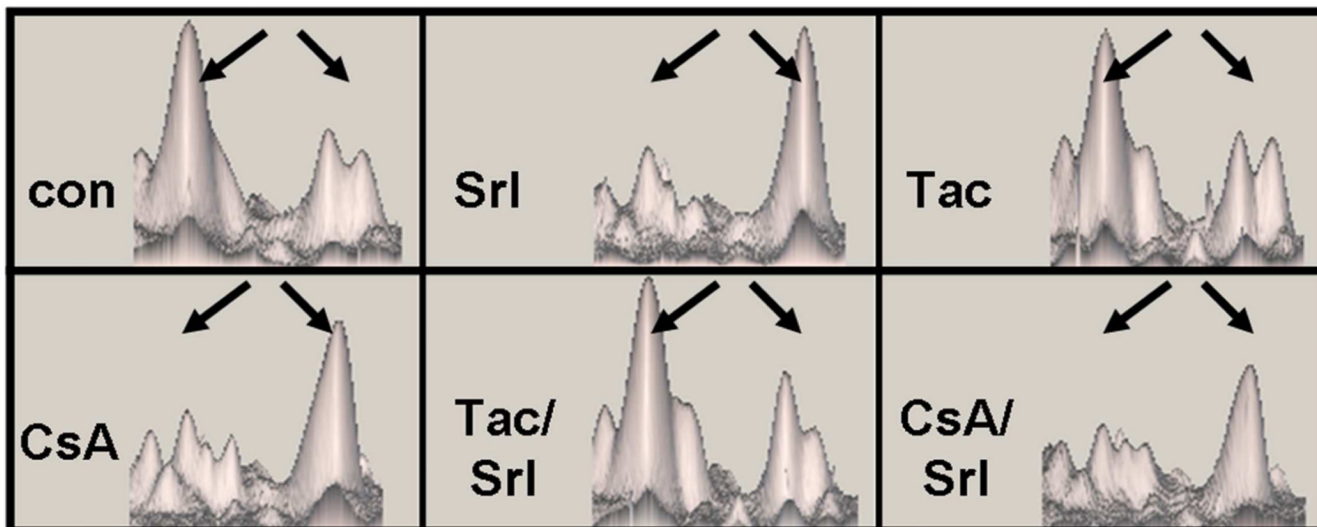


Figure 5. Immunosuppressant-induced changes of regucalcin compared to vehicle controls after 28 days of treatment

The two spots associated with regucalcin as displayed in the IMAGE-Master software are shown. The pI and molecular weight as detected on the gel matched the theoretical values of regucalcin (Figure 2). The spot at pH 4.35 and 33kDa (left spot) is markedly reduced after treatment with sirolimus, cyclosporine and cyclosporine + sirolimus. This is associated with the increase of volume of a corresponding spot (right) at the same molecular mass but at a different pH (4.25). Both spots were independently cut from the gel, digested and identified by HPLC/MS analysis. The right and left spots showed amino acid coverage of 41% and 38% with 10 and 9 distinct amino acids, respectively. Abbreviations: con: vehicle controls, CsA: 10 mg/kg/d cyclosporine, CsA/Srl: 10 mg/kg/d cyclosporine+ 1 mg/kg/d sirolimus, Srl: 1 mg/kg/d sirolimus, Tac: 1 mg/kg/d tacrolimus, Tac/Srl: 1 mg/kg/d tacrolimus + 1 mg/kg/d sirolimus.

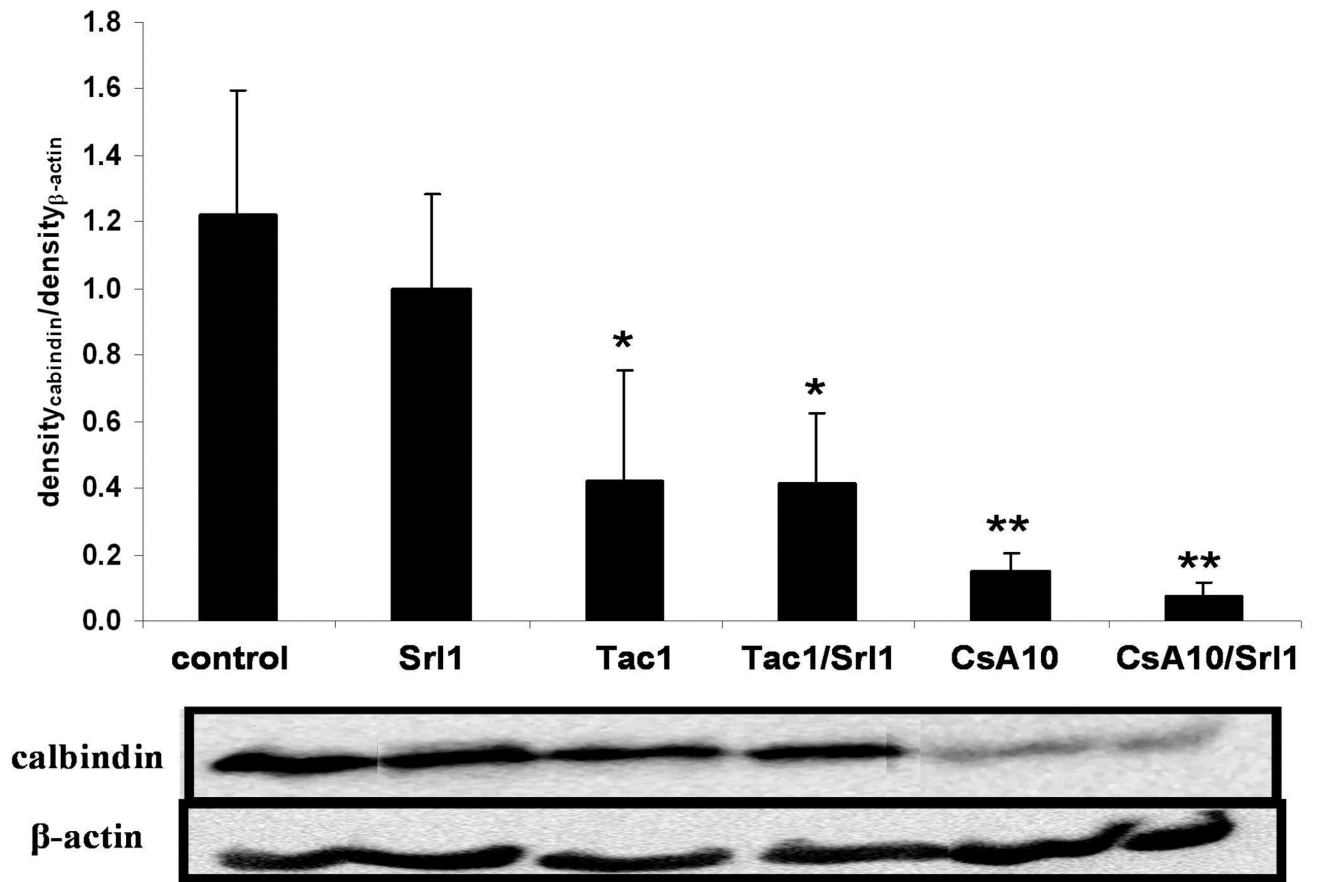


Figure 6. Comparison of calbindin-D_{28k} among treatment groups using Western blot analysis
 Analysis of variance: $p=0.00015$. Significance levels *: $p<0.05$; **: $p<0.001$; (Tukey method). β -Actin was used as control and was expected not to change. Abbreviations: CsA10: 10 mg/kg/d cyclosporine, CsA10+Srl1: 10 mg/kg/d cyclosporine+ 1 mg/kg/d sirolimus, Srl1: 1 mg/kg/d sirolimus, Tac1: 1 mg/kg/d tacrolimus, Tac1+Srl1: 1 mg/kg/d tacrolimus + 1 mg/kg/d sirolimus.

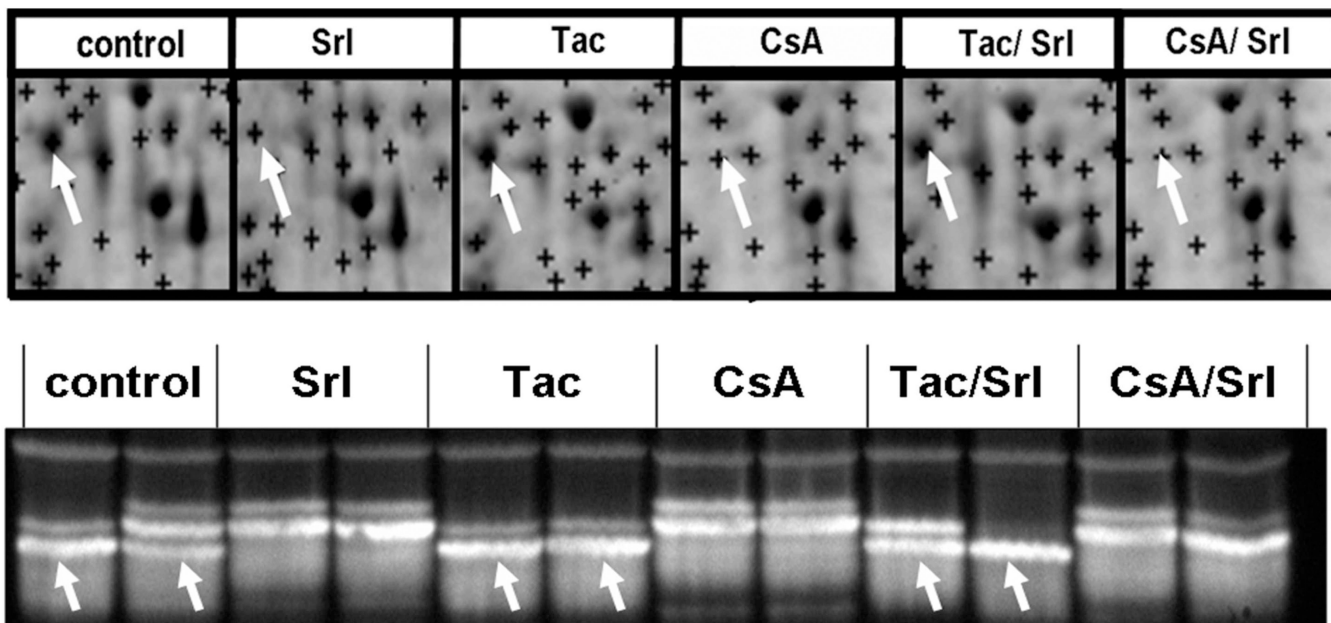


Figure 7. Comparison of the effects of treatment with immunosuppressants alone and in combination at the doses tested on NADH-ubiquinone oxidoreductase subunit 10 expression in the kidney

Top: Representative 2D-gel regions. The region at 38kDa and pH 6.1 corresponded to NADH-ubiquinone oxidoreductase subunit 10. Bottom: Western blot analysis of the Complex I of the respiratory chain, NADH-ubiquinone oxidoreductase subunit 10. Three different modifications of the subunit 10 were observed. Treatment with different immunosuppressants and their combination resulted in an alteration of the pattern as compared to the control group. The band at 38 kDa in the Western blots (bottom) is labeled with an arrow. The modifications have not yet been identified. The protein changes observed in the Western blots matched those after 2D-gel electrophoresis.

Immunosuppressant blood concentrations and kidney function parameters 4 hours after the last dose on day 28.

Table 1

	Blood concentrations			Glomerular function	
	Srl (ng/mL)	Tac (ng/mL)	CsA (ng/mL)	GFR [μL/100g rat]	Creatinine [mg/dL]
Control				358± 132	0.4± 0.1
Srl1	6.8± 0.4			266± 29	0.6± 0.1
Tac1		3.0± 2.3		246± 42	0.4± 0.1
Tac1+Srl1	9.1± 3.1	3.3± 2.4		208± 55	0.4± 0.1
CsA10			1112± 350	148± 68	0.7± 0.1
CsA10+Srl1	16.1± 5.9		1010± 140	50± 48	0.8± 0.1

All values are presented as means ± standard deviations (n=6). Abbreviations: CsA: cyclosporine, CsA10+Srl1: 10 mg/kg/d cyclosporine, CsA10+Srl1+ 1 mg/kg/d sirolimus, GFR: glomerular filtration rates as determined using the fluorescein isothiocyanate (FITC)-inuline method (26), Srl: sirolimus, Srl1: 1 mg/kg/d sirolimus, Tac: tacrolimus, Tac1: 1 mg/kg/d tacrolimus, Tac1+Srl1: 1 mg/kg/d tacrolimus + 1 mg/kg/d sirolimus. Creatinine concentrations were measured in plasma.

Immunosuppressant-induced changes in kidney protein expression compared to vehicle controls as estimated based on 2D-gels.

Table 2

Protein name	Acc. number	Score / AA-cov.	Changes compared to controls							MW on gel [kDa]	pI on gel [pH]	MW Theoretical [kDa]	pI Theoretical [pH]
			S	C	S/C	T	S/T	T					
vimentin	14389299	233 / 32%	↑*	↑*	↑*	↑*	=	=	=	56	4.9	54	5.1
caldesmon	6978589	175 / 25%	=	↑*	↑*	=	=	=	=	60	6.3	61	6.3
Prolyl-4-Hydroxylase	38197382	250 / 30%	=	↑*	↑*	=	=	=	=	50	4.9	60	4.8
Drebrin like protein	13786198	137 / 25%	↑*	↑*	↑*	=	=	↑	↑	50	4.9	48	4.9
Actinrelated Protein 3B	12835802	178 / 30%	↑	↑*	↑*	=	=	↑	↑	48	5.7	47	5.6
HSP 90 beta	34862435	282 / 23%	=	↑*	↑	=	=	=	=	47	4.7	92	4.7
Glycine amidinotransferase	13385454	91 / 20%	↓*	=	=	=	=	↓*	↓*	47	6.8	48	7.2
Angiogenin inhibitor	20806151	196 / 32%	=	↑*	↑	=	=	=	=	45	4.6	49	4.6
Kidney aminoacylase	50925537	273 / 50%	↑*	↑*	↑*	=	=	↑	↑	45	6.3	45	6.1
Catalase	6978607	176 / 23%	↑*	=	↑	↑	↑	↑*	↑*	40	6.1	59	7.5
Fructose-1,6-bisphosphatase	51036635	264 / 53%	=	↑*	↑*	=	=	=	=	39	5.6	40	5.5
NADH oxidoreductase	32996721	181 / 33%	↓↓*	↓↓*	↓↓*	=	=	=	=	38	6.0	40	7.1
Pyridoxal-(V.H.β)-kinase	13929082	209 / 51%	↑*	↑*	↑*	↑	↑	↑	↑	35	6.3	35	6.3
Pyruvate kinase	16757994	182 / 25%	↑*	↑	↑*	↑*	↑*	↑	↑	34	6.4	58	6.7
Regucalcin	13928740	160 / 41%	↓*	↓↓*	↓↓*	=	=	=	=	33	5.3	33	5.3
Isocitrate DH (NADP)	13928690	196 / 30%	↓↓*	↓*	↓*	=	=	=	=	33	6.7	47	6.6
alpha-2u-globulin, major urinary protein (7 spots)	22219450	100-180 / 21%-51%	↓*	↓*	↓*	=	=	=	=	22	5	20	5.8
GM2 activator Protein	25006237	95 / 18%	=	↑	↑*	=	=	↑	↑	~20	5.0	21	5.6
Proteasome subunit 3	8394082	87 / 34%	↑*	↑	↑*	=	=	↑	↑	~20	6.4	23	6.2
Calbindin-D	14010887	208 / 46%	=	↓↓*	↓↓*	↓	↓	↓	↓	25	4.6	28	4.7
TCTP p21	55562869	55 / 23%	↑	↑	↑*	↑	↑	↑	↑	~20	4.8	20	4.8
Plastin 3 T-isoform	34875362	378 / 39%	=	↑	↑*	↑	↑	↑	↑	~60	5.2	70	5.2

Protein name	Acc. number	Score / AA-cov.	Changes compared to controls						MW on gel [kDa]	pI on gel [pH]	MW Theoretical [kDa]	pI Theoretical [pH]
			S	C	S/C	T	S/T	T				
Aldehyde DH7 antiqumintin	34879551	228 / 28%	=	↑	↑	↓	↓	↓*	6.8	55	55	7
Aldose reductase	6978491	163 / 42%	=	=	=	↓	↓*	↓*	6.5	35	35	6.3
Ddah1 protein	38371755	177 / 45%	↑	=	↑	↑*	↑*	↑*	6.1	31	31	5.8
RICKEN cDNA 1810013B01	27721409	60 / 21%	=	=	=	=	=	↑*	5.4	24	22	5.6

* Arrows represent more than -30% (↓), -50% (↓↓), +40% (↑), +100% (↑↑) of change between the group averages in the density of protein spots as compared to untreated controls (significant changes p<0.05 [Tukey test pairwise comparison to controls]). Molecular weights (49), isoelectric points (pI) are shown both as measured on gels and as listed in the Swiss Prot and NCBI databases.

Abbreviations: AA-cov.: amino acid coverage, Acc. Numbers: NCBI accession number, C: cyclosporine, C/S: cyclosporine + sirolimus, S: sirolimus, T: tacrolimus, T/S: tacrolimus + sirolimus.

Table 3

Association between immunosuppressant-induced changes in the expression of proteins involved in energy metabolism (A), expression of kidney aminoacylase (B) and the urine concentrations of their corresponding substrates and/or products.

	Control	SrII	CsA10	CsA10 + SrII	TacI	TacI + SrII
A	Pre-TCA cycle [% of total integral]	13	144* [↑]	169* [↑]	189* [↑]	121* [↑]
	TCA cycle [% of total integral]	173	100* [↓]	121 [↓]	64* [↓]	129 [↓]
	Pyruvate kinase [% of control]	100	180* [↑]	160 [↑]	220* [↑]	140* [↑]
	NADH oxidoreductase [% of control]	100	30* [↓]	40* [↓]	30* [↓]	110
B	Hippurate [% of total integral]	47.2	15.0* [↓]	13.1* [↓]	4.7* [↓]	23.3 [↓]
	Kidney aminoacylase-1 [% of control]	100	165* [↑]	190* [↑]	195* [↑]	100
	α-glucose [% of total integral]	4.0	2.3	28.9* [↑]	117.0* [↑]	4.8
C	F-1,6-BP [% of control]	100	120	187* [↑]	171* [↑]	103
	Creatine [% of total integral]	6.0	28.6* [↑]	2.5	28.9* [↑]	3.7
D	AGAT [% of control]	100	61* [↓]	122	85	103
						74* [↓]

Arrows mark the direction of concentration changes.

* significant changes $p < 0.05$ (Tukey test pairwise comparison to controls).

Abbreviations: CsA10: 10 mg/kg/d cyclosporine, CsA10+SrII: 10 mg/kg/d cyclosporine+ 1 mg/kg/d sirolimus, SrII: 1 mg/kg/d sirolimus, TacI: 1 mg/kg/d tacrolimus, TacI+SrII: 1 mg/kg/d tacrolimus + 1 mg/kg/d sirolimus; Pre-TCA cycle metabolites: sum of lactate and acetate concentrations; TCA cycle metabolites: sum of succinate, citrate and 2-oxoglutarate concentrations; F-1,6-BP: Fructose-1,6-bisphosphatase, AGAT: Arginine-glycine-amidino transferase.